Radio-echo sounding at Dome C, Antarctica: A compilation of measured and modeled data

Anna Winter, Olaf Eisen, Daniel Steinhage

With contributions from BAS, CReSIS, INGV and UTIG

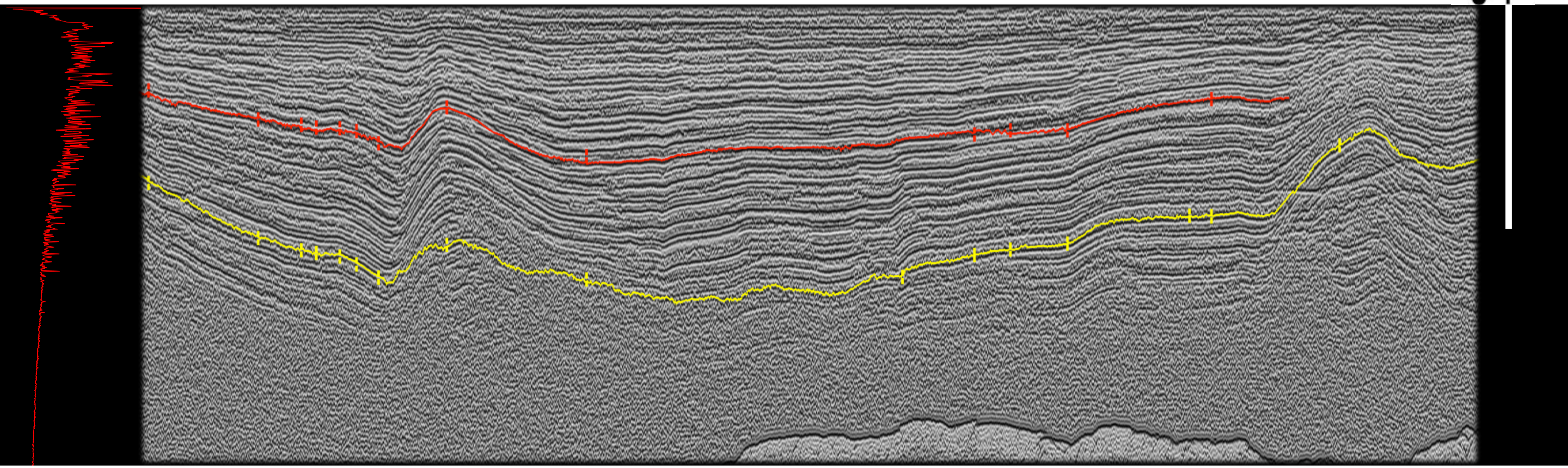

Outline

Dome C ice-core measurements of dielectric properties

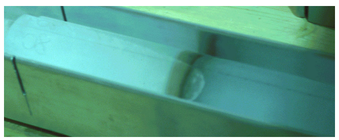

Radio-echo sounding (RES) profiles around drill site

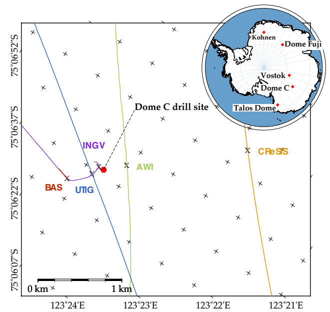

TWT to depth conversion via conductivity record and age assignment for identified IRHs

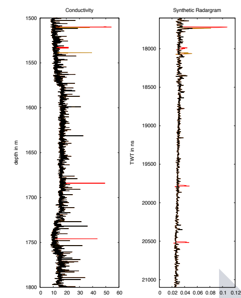

Synthetic radargrams from ice-core data

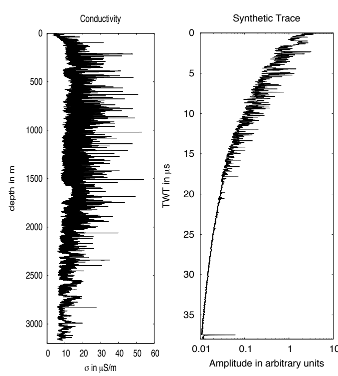

Compilation of all data, identification of common internal reflection horizons (IRHs)

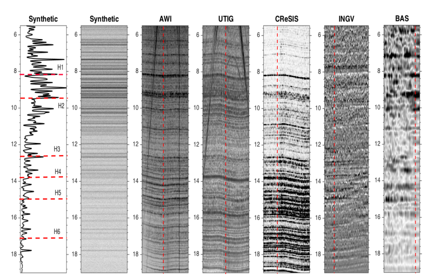

Results

- Comparability of various radar systems for Oldest Ice reconnaissance surveys
- Depth and age for conductivity-caused IRHs
- Starting point for isochronous IRH tracing and Dome C age structure extrapolation
- One step towards the Oldest-Ice ice core

HELMHOLTZ ASSOCIATION

Dome C ice-core data

Ice core

- EPICA Dome C, second ice core
- Located on East Antarctic Plateau
- Elevation: 3233 m a.s.l.
- Ice thickness: 3309 m
- Accumulation rate: 25 kg m^{-2} a^{-1}
- Mean annual surface temperature: -54.5°C
- Core length: 3260 m
- Maximum age: ~800 ka

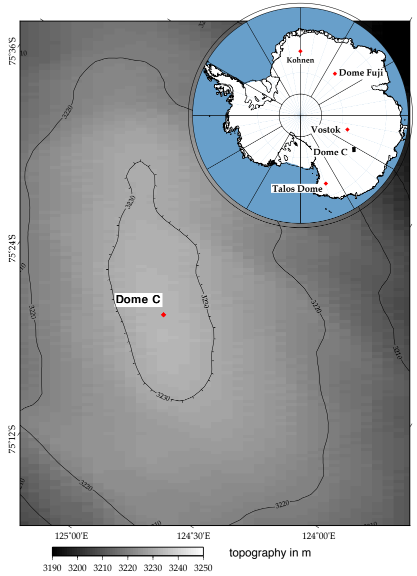

Location of Dome C on the East Antarctic Plateau and topography at the drill site.

Dielectric profiling (DEP) measurements

- DEP bench after Moore (1993)
- Conducted in the field
- Measurement at -20°C with 100 kHz
- Corrected to -15°C
- Conductivity profile from 6.8 m - 3165.2 m with 0.02 m steps

Density measurements

- γ-absorption method
- Conducted at Alfred Wegener Institute, Bremerhaven
- Density profile from 6.8 m - 112.7 m with 1 mm steps

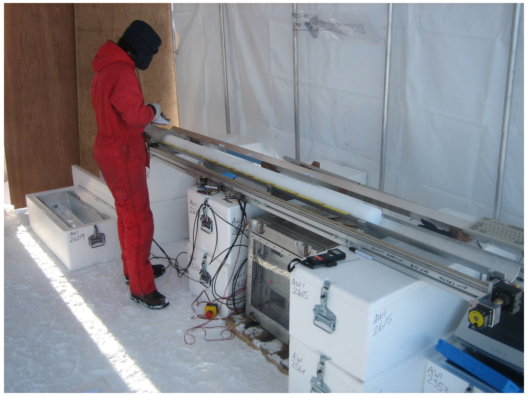

Synthetic traces

Measured density ρ is used to calculate the ordinary relative dielectric permittivity ε' with the real-valued dielectric mixture equation by Looyenga (1965):

$$\varepsilon'(z) = \left(\frac{\rho(z)}{\rho_{ice}} \left({\varepsilon'_{ice}}^{\frac{1}{3}} - 1 \right) + 1 \right)^3$$

with pure-ice values ρ_{ice} and ε'_{ice} .

Together with the conductivity σ this gives the complex relative permittivity:

$$\varepsilon = \varepsilon' - i\varepsilon'' = \varepsilon' - i \frac{\sigma}{\varepsilon_0 \omega}$$

This is the input for the 1D model 'emice' (Eisen et al., 2004), solving Maxwell's equations to calculate synthetic radar traces.

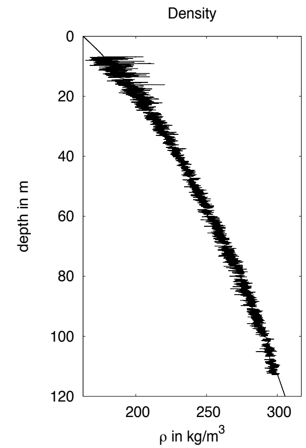

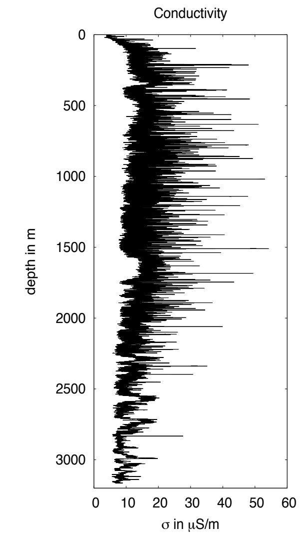

1D model of Maxwell's equations to calculate wave propagation

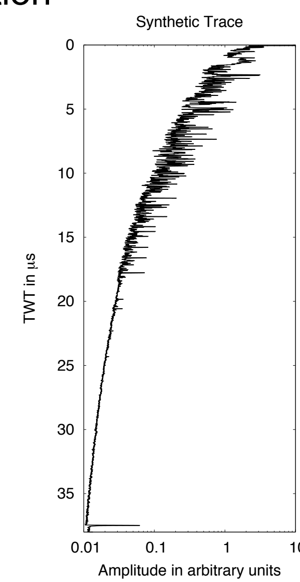

HELMHOLTZ ASSOCIATION

Radio-echo sounding (RES) data

- Electromagnetic waves are partly reflected at horizons of changing dielectric properties
- This leads to internal reflection horizons (IRHs), caused by
  - Density: isochronous, only in upper few hundred meters
  - Conductivity: isochronous, throughout ice column
  - Cristal orientation fabric: maybe isochronous, deeper parts of ice column

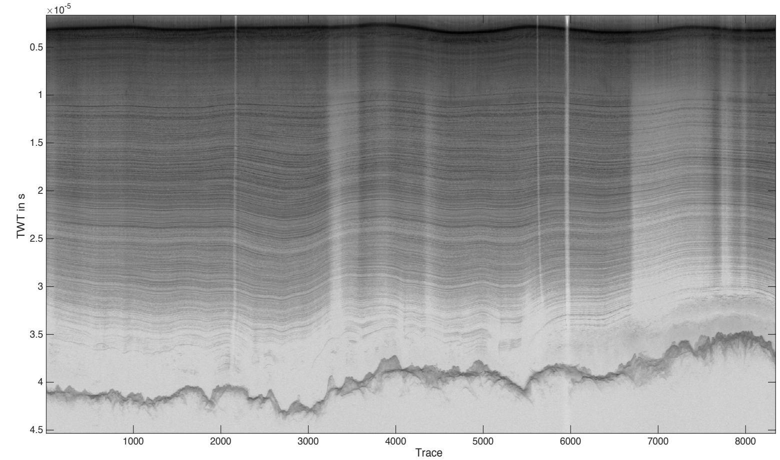

Radargram example of the CReSIS profile

- We use RES data of five different systems:
  - Alfred Wegener Institute (AWI), Germany
  - British Antarctic Survey (BAS), UK
  - Center for Remote Sensing of Ice Sheets (CReSIS), USA
  - Istituto Nazionale di Geofisica e Vulcanologia (INGV), Italy
  - University of Texas Institute for Geophysics (UTIG), USA
- Within 2 km from Dome C drill site

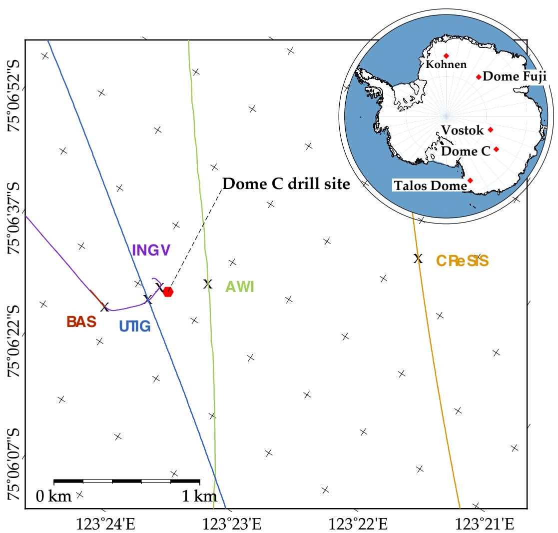

Positions of the five RES profiles with respect to the Dome C drill site.

Table 1: Characteristics of the five RES systems. The last row gives the best vertical resolution due to bandwidth (for distinguishing two reflectors), i.e. without taking into account any windowing of signals during processing.

System	aircraft	season	center freq. MHz	bandwidth/ pulse length	vertical sampl. freq. MHz	resolution m
AWI	DC-3T	2007/08	150	60 ns	75	5.0
BAS	Twin Otter	2005/06	150	10 MHz	22	8.4
CReSIS	Orion P3	2012/13	195	30 MHz	30	2.8
INGV	ground based	2011/12		200 ns	25	16.8
UTIG	DC-3T	2008/09	60	15 MHz	50	5.6

Data compilation

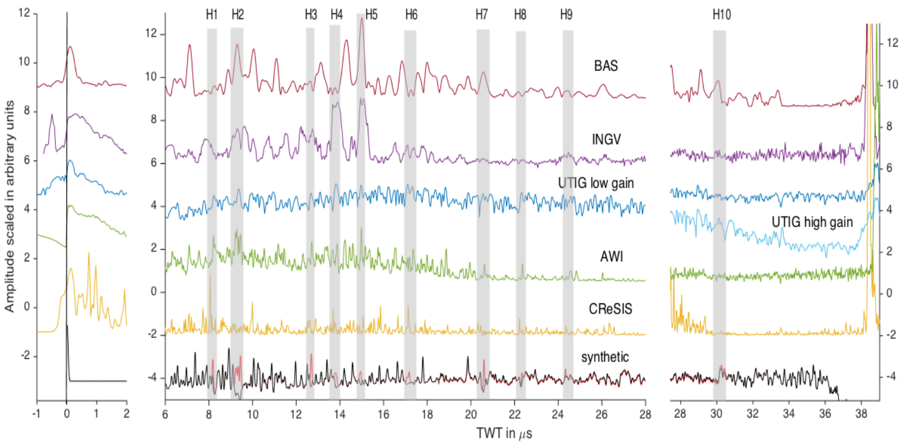

RES traces of the five radar systems and synthetic trace. The surface reflections are shifted to time zero (left panel). 10 reflections, distinct in most or all of the traces and used for depth conversion are gray-shaded.

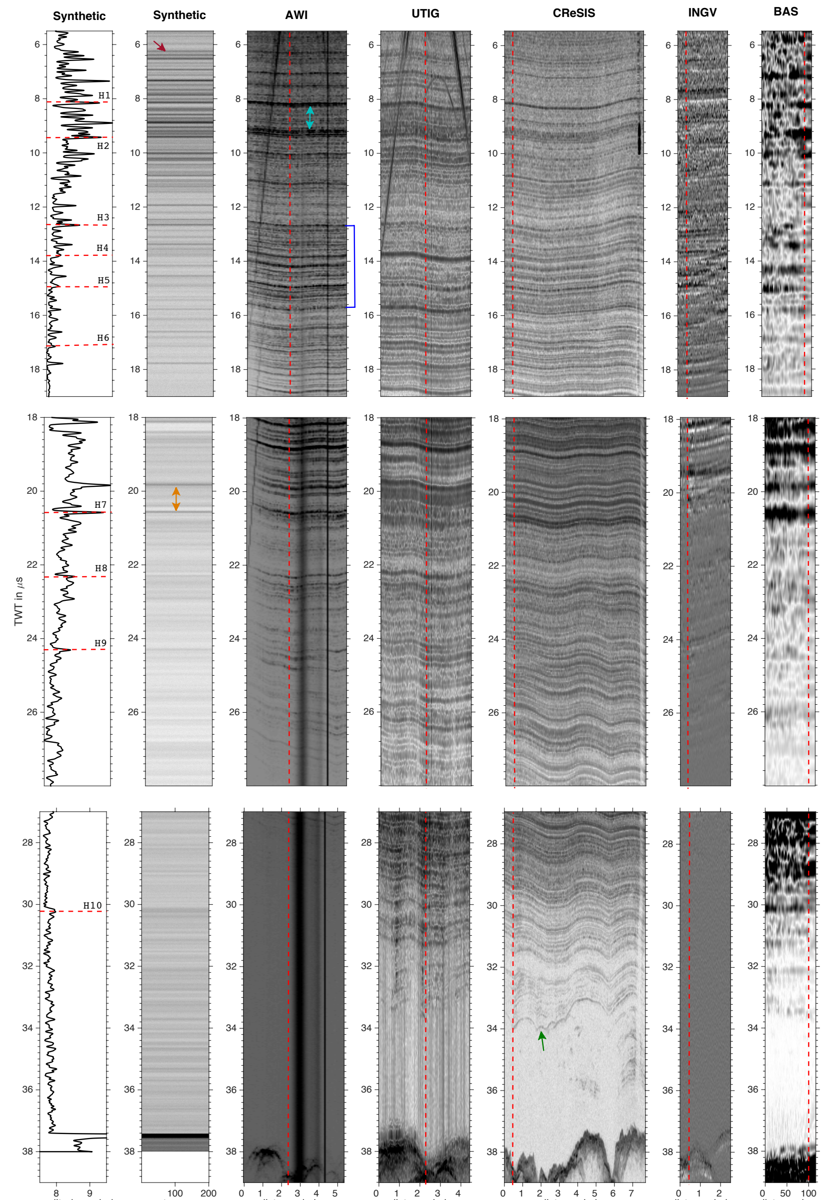

- Identification of 10 IRHs, comparable in synthetic and measured RES data
- Comparison of different RES data with respect to :
    - Resolution of internal reflectors
    - Spatial coherence of reflectors
    - Penetration depth
    - Quality of imaging the basal layer
    - Resolution of bedrock topography

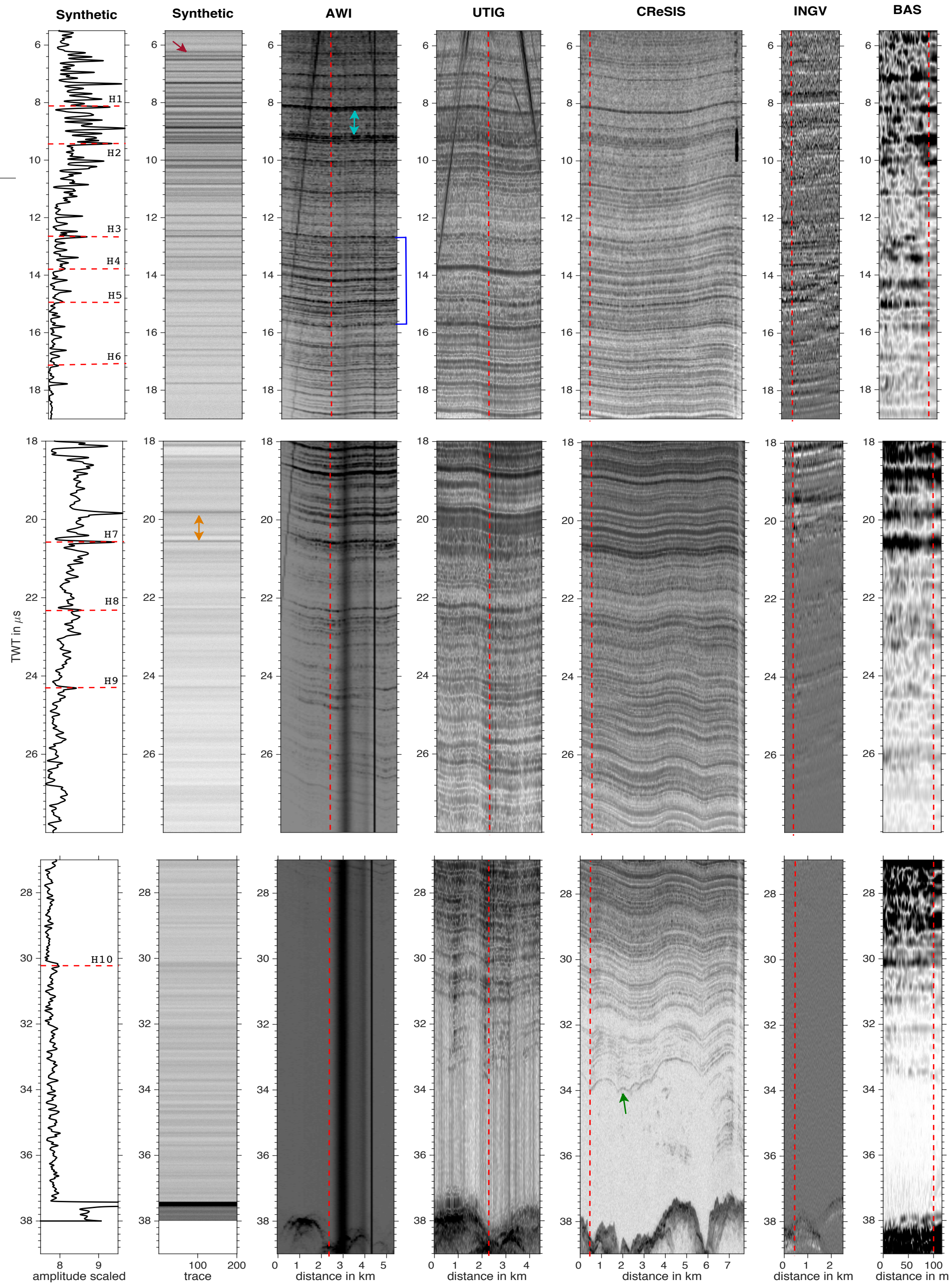

Z-scopes of synthetic and RES data sets. The horizontal red lines mark the gray-shaded identified reflections of the single-traces figure. The vertical lines give the positions of the single traces. Prominent features are marked by colored arrows.

Determination of IRH origin and ages

- Removal of signals from the conductivity record
- Model run with new conductivity profile
- Identified reflections are removed from synthetic trace

➡ Depth origin of reflectors is that of removed conductivity sections

- Age assignment from ice-core time scale (AICC2012)

➡ Accurate ages for IRHs in RES data, as they are matched with the synthetic reflections

➡ Identified IRHs are conductivity-caused and thus isochronous

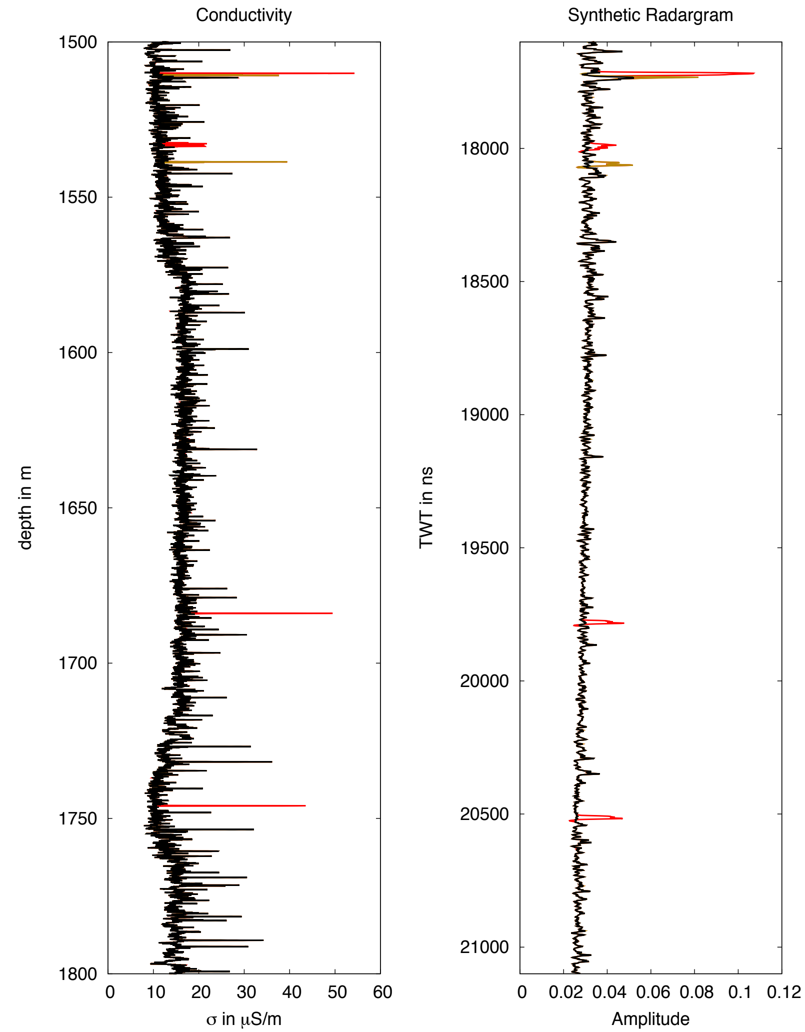

Results: Depth and age of IRHs

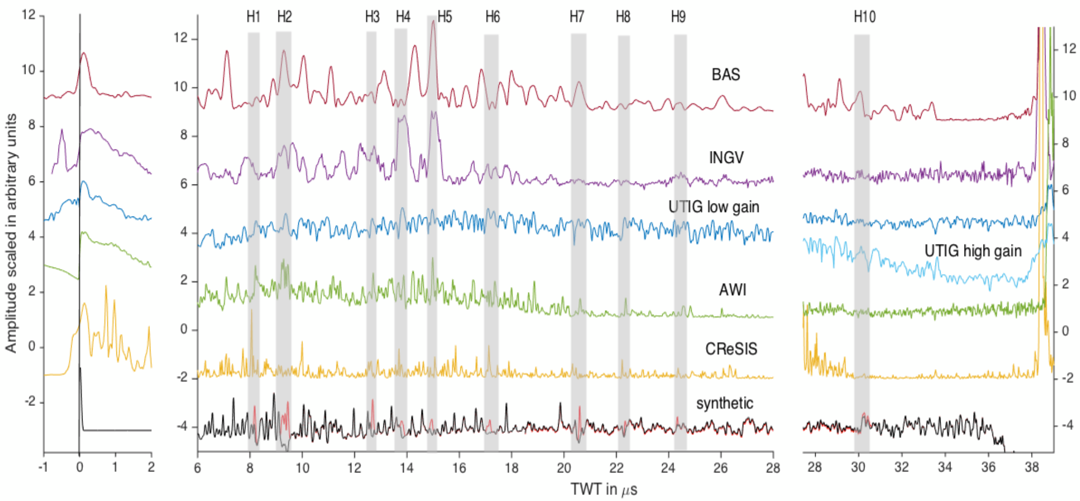

RES traces of the five radar systems and synthetic trace. The surface reflections are shifted to time zero (left panel). 10 reflections, distinct in most or all of the traces and used for depth conversion (table below) are gray-shaded.

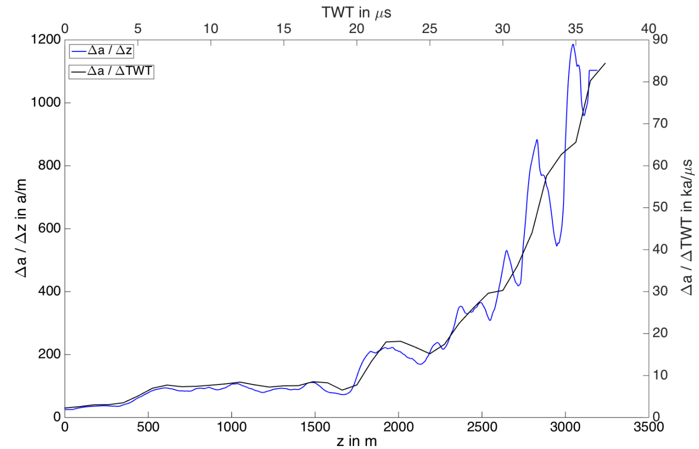

Change of age with depth / TWT on the AICC2012 time scale, Dome C to infer uncertainties due to reflection-peak widths or shifts

Horizon	TWT µs	depth top m	depth bottom m	age top ka	age bottom ka	σ_{age} ka
H1	8.0	700.54	702.64	38.17	38.30	0.58
H2	9.5	786.84	808.80	45.49	47.22	0.78
H3	12.5	1078.90	1081.36	73.66	73.96	2.00
H4	13.5	1172.04	1179.06	82.03	82.58	1.53
H5	15.0	1267.34	1271.30	90.04	90.40	1.60
H6	17.5	1447.58	1458.16	106.32	107.49	1.88
H7	20.5	1745.80	1746.02	132.74	132.22	2.13
H8	22.5	1891.54	1892.98	160.96	161.24	3.50
H9	24.5	2060.14	2060.40	197.17	197.23	1.96
H10	30.0	2549.88	2588.34	328.97	337.96	2.74

HELMHOLTZ ASSOCIATION